DAΦNE

The DAΦNE Team

D. Alesini, M.E. Biagini, C. Biscari, R. Boni, M. Boscolo, F. Bossi, B. Buonomo, A. Clozza, G. Delle Monache, T. Demma (Art. 23), E. Di Pasquale, G. Di Pirro, A. Drago, A. Gallo, A Ghigo, S. Guiducci, C. Ligi, F. Marcellini, C. Marchetti, G. Mazzitelli, C. Milardi, F. Murtas, L. Pellegrino, M. Preger, L. Quintieri (Art. 23), P. Raimondi (Resp.), R. Ricci, U. Rotundo, C. Sanelli, M. Serio, F. Sgamma, B. Spataro, A. Stecchi, A. Stella, S. Tomassini, C. Vaccarezza, P. Valente, M. Zobov

The DAΦNE Technical Staff

G. Baldini, P. Baldini, A. Battisti, A. Beatrici, M. Belli, B. Bolli, L. Cacciotti, G. Ceccarelli, R. Ceccarelli, A. Cecchinelli, S. Ceravolo, R. Clementi, O. Coiro, P. Ciuffetti, S. De Biase, I. De Cesaris, M. De Giorgi, R. Di Raddo, M. Di Virgilio, A. Donkerlo, G. Ermini, M.R. Ferrazza, G. Fontana, U. Frasacco, C. Fusco, F. Galletti, E. Gaspari, M. Giabbai, O. Giacinti, E. Grossi, F. Iungo, V. Lollo, M. Marchetti, C. Marini, M. Martinelli, A. Mazzenga, C. Mencarelli, M. Monteduro, M. Paris, E. Passarelli, V. Pavan, S. Pella, D. Pellegrini, G. Piermarini, S. Quaglia, F. Ronci, M. Rondinelli, F. Rubeo, M. Sardone, M. Scampati, G. Sensolini, R. Sorchetti, A. Sorgi, M. Sperati, A. Sprecacenere, P. Tiseo, R. Tonus, T. Tranquilli, M. Troiani, V. Valtriani, R. Zarlenga, A. Zolla

DAΦNE is an electron-positron Φ-*meson factory* operating at Frascati since 1997. Factories are storage ring colliders designed to work at the energies of the meson resonances, where the production cross section peaks, to deliver a high rate of events to high resolution experiments.

The factory luminosity (the number of events per unit time produced by the reaction under investigation divided by its cross section weighted by the acceptance of the detector) is very high, about two orders of magnitude larger than that obtained at the same energy in colliders of the previous generation. One of the key-points to get a substantial luminosity increase is the use of separated vacuum chambers for the two beams merging only in the interaction regions (IRs). When sharing the same ring the two N-bunch trains cross in 2N points and the maximum luminosity is limited by the electromagnetic beam-beam interaction. The unwanted effects of this interaction can be reduced with a very strong focussing (called "low-β") at the interaction point (IP), obtained by means of quadrupole doublets or triplets. However these magnetic structures take up much space and excite chromatic aberrations which must be corrected elsewhere in the ring.

This limitation does not hold for the double ring option, consisting in two separate rings crossing at two low-β points. The number of bunches that can be stored in such a collider is limited only by the geometry of the IR's.

DAΦNE is an accelerator complex consisting of a double-ring collider, a linear accelerator (LINAC), an intermediate damping ring to make injection easier and faster and 180 m of transfer lines connecting these machines. The beam accelerated by the Linac can also be switched into a laboratory called "Beam Test Facility (BTF)", for dedicated experiments and calibration of detectors. Three synchrotron radiation lines, two from bending dipoles and the other from the wiggler are routinely operated by the DAΦNE-LIGHT group in a parasitic mode, providing photons from the infrared to soft x-rays.

1 Injection System

In a low energy electron-positron collider, such as DAΦNE, the lifetime of the stored current is mainly limited by the Touschek effect, namely the particle loss due to the scattering of the particles inside the bunches. In the present typical operating conditions the Touschek lifetime is below 1000 s. It is therefore necessary to have a powerful injection system, capable of refilling the beam without dumping the already stored one. In addition, flexibility of operation requires that any bunch pattern can be stored among the 120 available buckets. The injection system of DAΦNE is therefore designed to deliver a large rate of particles in a single bunch at the working energy of the collider.

It consists of a linear accelerator with a total accelerating voltage of 800 MV. In the positron mode, electrons are accelerated to $\approx$ 250 MeV before hitting a tungsten target (called positron converter) where positrons are generated by bremsstrahlung and pair production with an efficiency of $\approx$1%. The positrons exit from the target with an energy of few MeV and are then accelerated by the second section of the LINAC to their final energy of $\approx$ 0.51 GeV. The positrons are then driven along a transfer line and injected into a small storage ring, called Accumulator, at frequency of 50 Hz. Up to 15 positron pulses are stacked into a single bucket of the Accumulator, then injection stops and the bunch damps down to its equilibrium beam size and energy spread, which are much smaller than the LINAC ones. Damping takes $\approx$ 0.1 s and then the beam is extracted from the Accumulator and injected into the positron main ring at an overall repetition rate of 2 Hz. A powerful and flexible timing system allows the storage of any desired bunch pattern in the collider. In the electron mode, a magnetic chicane deviates the particle trajectory around the positron converter and electrons are directly accelerated to 0.51 GeV and injected into the Accumulator in the opposite direction with respect to positron operation. They are then extracted like in the positron case and injected into the electron main ring through the second transfer line.

The Accumulator ring has been introduced in the accelerator complex to increase the injection efficiency, especially for the positrons that are produced by the LINAC at 50 Hz rate in 10 ns pulses with a charge of $\approx$ 0.5 nC. Since the design charge of the main ring at the maximum luminosity is $\approx$ 1.5 μ C and the longitudinal acceptance of the main rings is only 2 ns, the number of 50 Hz pulses necessary to fill the ring is of the order of 10^4. In order to avoid saturation it is therefore necessary that at each injection pulse a fraction smaller than 10^{-4} of the already stored beam is lost, and this is not easy to achieve. The Accumulator instead works with a lower frequency RF cavity and therefore with a larger longitudinal acceptance. In this way the full charge coming from the LINAC can be stored in a single RF bucket. In a complete injection cycle, that has a duration of 500 ms, up to 15 LINAC pulse can be stored in a single Accumulator RF bucket, and after being damped to the ring equilibrium emittances and energy spread, the whole stacked charge can be stored into a single RF bucket of the main ring. In this way the nominal single bunch charge can be stored with only one pulse from the Accumulator, reducing to 120 the number of injection pulses (at 2 Hz) into each main ring. As an additional benefit, the transverse beam size and energy spread of the beam coming from the Accumulator are at least one order of magnitude smaller than those of the LINAC beam, and this strongly reduces the aperture requirements of the main ring and, as a consequence, the overall cost of the collider.

2 Main Rings

In the DAΦNE collider the two beam trajectories cross at the interaction point (IP) with an horizontal angle that has been recently increased from ≈ 25 mrad to ≈ 50 mrad. A positron bunch leaving the IP after crossing an electron one will reach the following electron bunch at a distance of half the longitudinal separation between bunches from the IP.

Due to the horizontal angle between the trajectories of the two beams, the distance in the horizontal direction between the two bunches is equal to the horizontal angle times half the longitudinal distance between the bunches in each beam. The beam-beam interaction can be harmful to the beam stability even if the distance in the horizontal direction between bunches of opposite charge is of the order of few bunch widths at points where the β function is high and this sets a lower limit on the bunch longitudinal separation and therefore on the number of bunches which can be stored in the collider. However, the so called *crab waist collision scheme* (CW) recently implemented in the machine alleviates this problem, as it will be exhaustively explained in the following of this report.

By design the minimum bunch separation at DAΦNE has been set to ≈ 80 cm, and the maximum number of bunches that can be stored in each ring is 120. This number determines the frequency of the radiofrequency cavity which restore at each turn the energy lost in synchrotron radiation, which must be 120 times the ring revolution frequency. The luminosity of the collider can therefore be up to 120 times larger than that obtainable in a single ring with the same size and optical functions. Crossing at an angle could in principle be a limitation to the maximum single bunch luminosity. In order to make the beam-beam interaction less sensitive to this parameter and similar to the case of single ring colliders where the bunches cross head-on, the shape of the bunches at the IP is made very flat (typical ranges of r.m.s. sizes are $15 \div 30$ mm in the longitudinal direction, $0.2 \div 1.5$ mm in the horizontal and $2.5 \div 10$ μm in the vertical one). The double ring scheme with many bunches has also some relevant challenges: the total current in the ring reaches extremely high values (5 A in the DAΦNE design, ≈ 1.4 A in the DAΦNE operation so far) and the high power emitted as synchrotron radiation needs to be absorbed by a complicated structure of vacuum chambers and pumping systems in order to reach the very low residual gas pressure levels necessary to avoid beam loss. In addition, the number of possible oscillation modes of the beam increases with the number of bunches, calling for sophisticated bunch-to-bunch feedback systems.

The double annular structure of the DAΦNE collider as it is now after the recent modifications to implement the crab waist scheme is shown schematically in Fig. 1. Both rings lay in the same horizontal plane and each one consists of a long external arc and a short internal one. Starting from the IP the two beams share the same vacuum chamber while traveling in a common permanent magnet defocusing quadrupole (QD) which, due to the beam off-axis trajectory increases the deflection of the two beam trajectories to ≈ 75 mrad. Shortly after the QD, at a distance of ≈ 82 cm from the IP, the common vacuum chamber splits in two separated ones connected to the vacuum chambers of the long and short arcs. Two individual permanent magnet quadrupoles (QFs) are placed just after the chamber separation. Together with the previous QD they constitute the low-β doublets focusing the beams in the IP. The long and short arcs consist of two "almost achromatic" sections (deflecting the beam by $\approx 85.4^{\circ}$ in the short arc and $\approx 94.6^{\circ}$ in the long one) similar to those frequently used in synchrotron radiation sources, with a long straight section in between. Each section includes two dipoles, three quadrupoles, two sextupoles and a wiggler. This

structure is used for the first time in an electron-positron collider and it has been designed to let DAΦNE deal with high current beams.

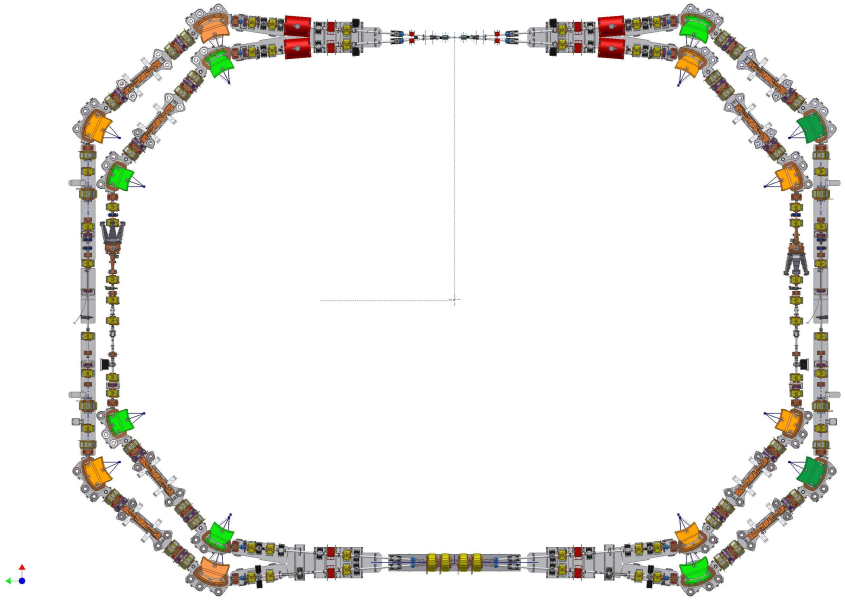

Figure 1: The DAΦNE Main Rings.

The amount of synchrotron radiation power emitted in the wigglers is the same as in the bending magnets and the wigglers can be used to change the transverse size of the beams. The increase of emitted power doubles the damping rates for betatron and synchrotron oscillations, thus making the beam dynamics more stable, while the possibility of changing the beam sizes makes the beam-beam interaction parameters more flexible.

The straight section in the long arc houses the kickers used to store into the rings the bunches coming from the injection system, while in the short straight arc there are the radiofrequency cavity and the equipment for the feedback systems which are used to damp longitudinal and transverse instabilities. The vacuum chambers of the arcs have been designed to stand the nominal level of radiation power emitted by the beams (up to 50 kW per ring). They consist of 10 m long aluminum structures built in a single piece: its cross section exhibits a central region around the beam and two external ones, called the antechambers, connected to the central one by means of a narrow slot. In this way the synchrotron radiation hits the vacuum chamber walls far from the beam and the desorbed gas particles can be easily pumped away. The chambers contain water cooled copper absorbers placed where the radiation flux is maximum: each absorber has a sputter ion pump below and a titanium sublimation pump above.

The Main Rings have undergone many readjustments during the years to optimize the collider performances while operating for different detectors.

In principle the rings could host two experiments in parallel, but only one at a time has been installed so far. Three detectors, KLOE, DEAR and FINUDA, have taken data until 2007 and logged a total integrated luminosity of ≈ 4.4 fb^{-1} with a peak luminosity of $\approx 1.6 \times 10^{32}$ cm^{-2}s^{-1} and a maximum daily integrated luminosity of ≈ 10 pb^{-1}.

KLOE has been in place on the first IP from 1999 to 2006, while DEAR and FINUDA have alternatively run on the second one. The detectors of KLOE and FINUDA are surrounded by large superconducting solenoid magnets for the momentum analysis of the decay particles and their magnetic fields represent a strong perturbation on the beam dynamics. This perturbation tends to induce an effect called "beam coupling", consisting in the transfer of the betatron oscillations from the horizontal plane to the vertical one. If the coupling is not properly corrected, it would give a significant increase of the vertical beam size and a corresponding reduction of luminosity.

For this reason two superconducting anti-solenoid magnets are placed on both sides of the detector with half its field integral and opposite sign, in this way the overall field integral in the IR vanishes.

The rotation of the beam transverse plane is compensated by rotating the quadrupoles in the low-β section. In the case of KLOE the low-β at the IP was originally designed with two quadrupole triplets built with permanent magnets, to provide high field quality and to left room to the detector.

The structure of the FINUDA IR is quite similar to the KLOE one. Since its superconducting solenoid magnet has half the length (but twice the field) of the KLOE one, the low-β focusing at the IP was obtained by means of two permanent magnet quadrupole doublets inside the detector and completed with two other conventional doublets outside.

The DEAR experiment, which was installed on the IR opposite to KLOE, took data during the years 2002-2003. It does not need magnetic field and therefore only conventional quadrupoles were used for the low-β. FINUDA rolled-in at DEAR's place in the second half of 2003 and took data until spring 2004. It was then removed from IP2 in order to run the KLOE experiment with only one low-β section at IP1, and rolled-in back in 2006 for a second data taking run ended in June 2007. After that the detector has been rolled-out again, and presently there are no detectors installed in IR2. The two chambers are vertically separated so that the two beams do not suffer from parasitic interactions in the whole IR2. A summary of the peak luminosity during these runs is shown in Fig. 2.

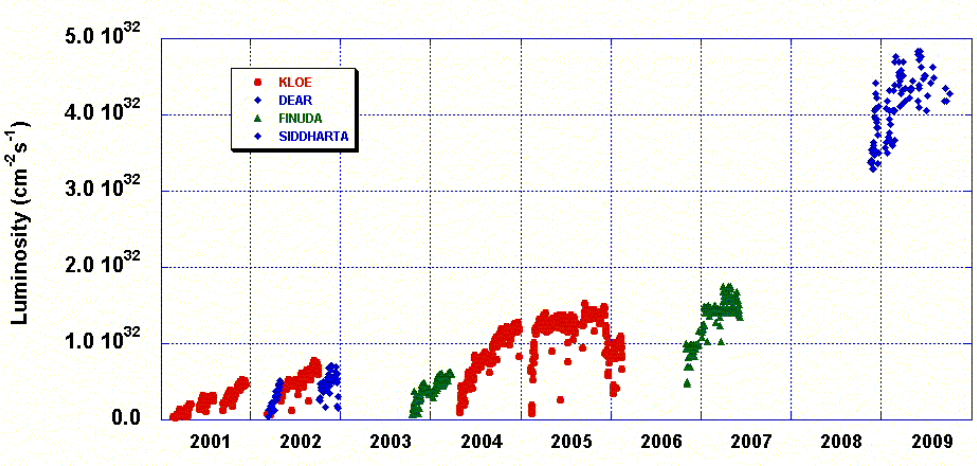

Figure 2: Peak luminosity at DAΦNE.

3 The large Piwinski angle and crab waist collision scheme at DAΦNE

In standard high luminosity colliders the key requirements to increase the luminosity are: very small vertical beta function β_y at the IP, high beam intensity I, the small vertical emittance ϵ_y and large horizontal beam size σ_x and horizontal emittance ϵ_x required to minimize beam-beam effects. The minimum value of β_y is set by the bunch length to avoid the detrimental effect on the luminosity caused by the hour-glass effect. It is very difficult to shorten the bunch in a high current ring without exciting instabilities. Moreover, high current implies high beam power losses, beam instabilities and a remarkable enhancement of the wall-plug power.

In the CW scheme of beam-beam collisions a substantial luminosity increase can be achieved without bunch length reduction and with moderate beam currents.

For collisions under a crossing angle θ the luminosity L and the horizontal ξ_x and vertical ξ_y tune shifts scale as:

$$L \propto \frac{N\xi_y}{\beta_y} \propto \frac{1}{\sqrt{\beta_y}}\,, \quad \xi_y \propto \frac{N\sqrt{\beta_y}}{\sigma_z\theta}\,, \quad \xi_x \propto \frac{N}{(\sigma_z\theta)^2} \tag{1}$$

The Piwinski angle ϕ is a collision parameter defined as:

$$\phi = \frac{\sigma_z}{\sigma_x}\tan\left(\frac{\theta}{2}\right) \approx \frac{\sigma_z}{\sigma_x}\frac{\theta}{2} \tag{2}$$

with N being the number of particles per bunch. Here we consider the case of flat beams, small horizontal crossing angle $\theta << 1$ and large Piwinski angle $\phi >> 1$.

In the large Piwinski angle and crab waist scheme described here, the Piwinski angle is increased by decreasing the horizontal beam size and increasing the crossing angle. In such a case, if it were possible to increase N proportionally to $\sigma_z\theta$, the vertical tune shift ξ_y would remain constant, while the luminosity would grow proportionally to $\sigma_z\theta$. Moreover, the horizontal tune shift ξ_x would drop like $1/\sigma_z\theta$. However, the most important effect is that the overlap area of the colliding bunches is reduced, as it is proportional to σ_x/θ (see Fig. 3). Then, the vertical beta function β_y can be made comparable to the overlap area size (i.e. much smaller than the bunch length):

$$\beta_y \approx \sigma_x/\theta << \sigma_z \tag{3}$$

We get several advantages in this case:

- Small spot size at the IP, i.e. higher luminosity L.
- Reduction of the vertical tune shift ξ_y with synchrotron oscillation amplitude.
- Suppression of synchrobetatron resonances.

There are also additional advantages in such a collision scheme: there is no need to decrease the bunch length to increase the luminosity as proposed in standard upgrade plans for B- and Φ-factories. This will certainly help solving the problems of HOM heating, coherent synchrotron radiation of short bunches, excessive power consumption etc. Moreover, parasitic collisions (PC) become negligible since with higher crossing angle and smaller horizontal beam size the beam separation at the PC is large in terms of σ_x.

However, large Piwinski angle itself introduces new beam-beam resonances which may strongly limit the maximum achievable tune shifts. At this point the crab waist transformation enters the game boosting the luminosity, mainly because of the suppression of betatron (and synchro-betatron) resonances arising (in collisions without CW) through the vertical motion modulation by the horizontal oscillations. The CW vertical beta function rotation is provided by sextupole magnets placed on both sides of the IP in phase with the IP in the horizontal plane and at $\pi/2$ in the vertical one (see Fig. 3).

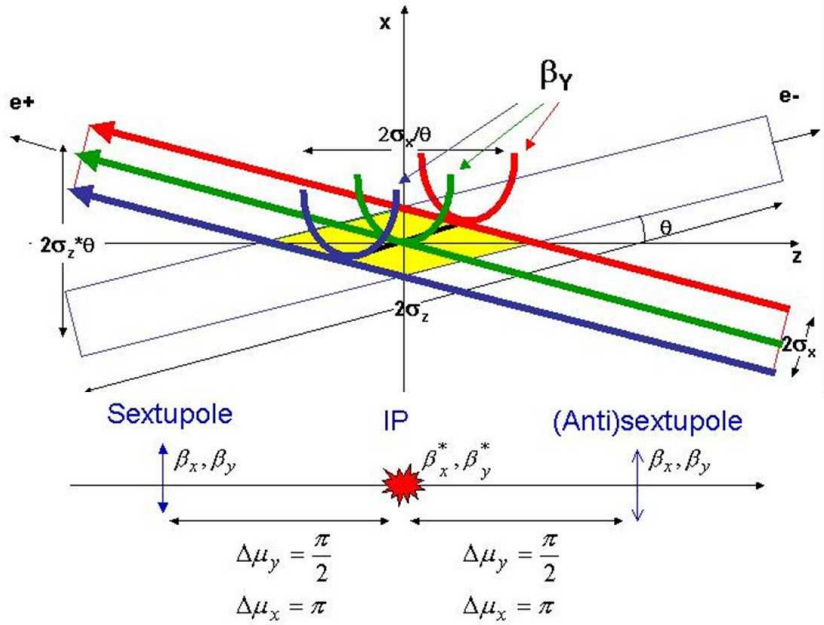

Figure 3: Crab waist scheme

For comparison, the parameters used during the last DAΦNE run with the KLOE detector (2005-2006) are shown in Table 1. As discussed above, in order to realize the CW scheme in

Table 1: DAΦNE Beam parameters for KLOE (2006) and SIDDHARTA (2008-2009)

PARAMETERS	KLOE Run	SIDDHARTA Run
L [cm^{-2}s^{-1}]	$1.5 \cdot 10^{32}$	$4.5 \cdot 10^{32}$
N_{part}/bunch	$2.65 \cdot 10^{10}$	$2.65 \cdot 10^{10}$
I_{bunch} [mA]	13	13
ϵ_x [10^{-9} m $\cdot$ rad]	340	260
ϵ_y [10^{-9} m $\cdot$ rad]	1.5	1
σ_x [μm]	760	200
σ_y [μm]	5.4	3.5
σ_z [mm]	25	17
β_x^* [m]	1.7	0.25
β_y^* [mm]	17	9
θ [mrad]	2×12.5	2×25

DAΦNE, the Piwinski angle ϕ should be increased and the beam collision area reduced: this is achieved by increasing the crossing angle θ by a factor 2 and reducing the horizontal beam size σ_x. In this scheme the horizontal emittance ϵ_x is reduced by a factor 1.5, and the horizontal beta function β_x lowered from 1.5 to 0.2 m. Since the beam collision length decreases proportionally to σ_x/θ, the vertical beta function β_y can be also reduced by a factor 3, from 1.8 cm to 0.6 cm. All other parameters are similar to those already achieved at DAΦNE.

4 Hardware upgrades for the Crab Waist test at DAΦNE

DAΦNE has been upgraded to allow the CW collision scheme test with the SIDDHARTA run during the summer shutdown of 2007.

The major upgrades on the machine are summarized as:

- new IR1 geometry for the CW test;
- new IR2 geometry with two completely separated vacuum chambers with half moon profile;
- new shielded bellows;
- the four e^+ e^- transverse feedbacks have been upgraded;
- solenoid windings in the two long IRs sections of the e^+ ring;
- new calorimeter for luminosity measurement and tuning;
- new longitudinal position of the two IRs horizontal collimators;
- new injection kickers.

The need of a new IR geometry is essentially due to have a very small β_y (9 mm) and a large crossing angle (25 mrad per beam). Splitter magnets installed in the original design have been removed thanks to the large crossing angle in the CW scheme. Defocusing and focusing quadrupoles (QD, QF) on both sides of the IP have been placed to obtain the required low-β structure. Further trajectory separation is provided by two small dipole correctors upstream and downstream the quadrupole doublets, while other three quadrupoles are used to match the betatron functions in the arcs.

The low-β section quadrupoles near the IP are of permanent magnet (PM) type. The QDs are located near the IP where the beams share a common vacuum chamber, while the QFs are positioned where the chambers are splitted and each one acts on a single beam. Therefore a total of two QDs and four QFs is required to get the two doublets around IP1. Four corrector dipoles provide a deflection of 9.5 mrad to match the inlet and outlet arc chamber flanges. CW sextupoles are placed at $\sim$ 9.3 m far from the IP1. Bending dipoles facing the IRs have been rotated and their field adjusted according to requirements. They have been powered with independent supplies to match these requirements.

For the SIDDHARTA experiment a new aluminium alloy (AL6082T6) chamber with two thin windows (0.3 mm 0.02 thickness) in the top and bottom sides has been designed and built.

Electromagnetic simulations have shown the presence of trapped modes which add resonant contributions to the beam coupling impedance in the Y-chamber junctions, the regions where the

two separate ring pipes merge in the common vacuum chamber near the IP. In the worst possible scenario, that occurs when a beam spectrum line at a frequency equal to a multiple to the bunch repetition rate is in full coupling, the joule loss does not exceed 200 W. To keep this effect under control the Y-chambers have been equipped with cooling pipes.

This additional cooling circuit allows to remove the beam induced HOM heating and, if necessary, to reduce it by detuning the mode frequencies with respect to the dangerous beam spectrum lines.

A new design of the central IR2 beam pipe has been implemented, the two vacuum chambers are completely separated and their cross section has an half moon profile.

In order to ensure a fast, accurate and absolute measurement of the luminosity and to fully understand the background conditions, the new interaction region has been equipped with three different luminosity monitors (Fig. 4): a Bhabha calorimeter, a Bhabha GEM tracker and a gamma Bremsstrahlung proportional counter. Different processes are used to measure luminosity:

- the Bhabha elastic scattering $e^+e^- \rightarrow e^+e^-$: it has a very clean signature (two back-to-back tracks); the available angle is limited due to the presence of the low-β quadrupoles, however, in the actual polar angle range covered by our calorimeters, 18° - 27°, the expected rate ($\sim$ 440 Hz at a luminosity of $10^{32}\text{cm}^{-2}\text{s}^{-1}$ is high enough and the backgrounds low enough to allow an online clean measurement;

- the very high rate of the radiative Bhabha process $e^+e^- \rightarrow e^+e^-\gamma$: it has the advantage that 95% of the signal in contained in a cone of 1.7 mrad aperture, but it suffers heavily from beam losses due to interactions with the residual gas in the beam-pipe, Touschek effect, and particles at low angles generated close to IR;

- the resonant decay $e^+e^- \rightarrow \Phi \rightarrow K^+K^-$: a rate of about 25 Hz at 10^{32} is expected in the SIDDHARTA experiment monitor at $\approx 90^o$.

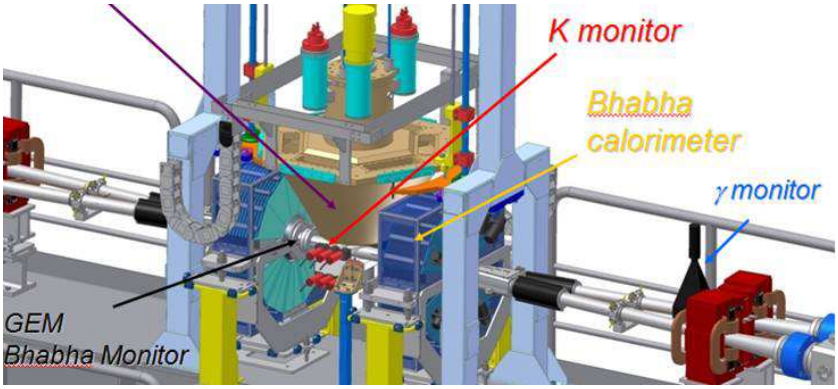

Figure 4: Overview of the upgraded DAΦNE IR1 showing the various luminosity detectors.

The main Bhabha monitor consists of a 4-modules sandwich calorimeter, made of lead and scintillator. Four modules of calorimeters surround the final permanent quadrupole magnets,

located at a distance of 32.5 cm on both sides of the IR, as shown in Fig. 4. They cover an acceptance of 18° - 27° in polar angle, and are segmented in azimuthal angle in five sectors, 30° wide.

Two gamma monitor detectors are located 170 cm away from the IR, collecting the photons radiated by electron or positron beam. The detectors are now made of four PbW04 crystals (squared section of 30×30 mm^2 and 110 mm high) assembled together along z, in order to have a 30 mm face towards the photon beam, and a total depth of 120 mm corresponding to about 13 X_0. Thanks to the high rate, those detectors are mainly used as a fast feedback for the optimization of machine luminosity versus background, since the relative contribution of background is changing with the machine conditions. A total systematic uncertainty on the luminosity measurement of 11% can be estimated.

5 Luminosity achievements during 2009

The commissioning of the upgraded machine started in November 2007. At the end of the year the ring vacuum was almost recovered, the beams were stored in the upgraded rings, all the sub-systems went quickly to regime operation.

The first collisions in the CW scheme have been obtained in February 2008, with the first experimental confirmation of the potentiality of the new configuration in terms of specific luminosity growth and reduction of the beam-beam detrimental effects.

Fig. 5 (top) reports integrated luminosity for each month during 2009 and Fig. 5 (bottom) shows the averaged daily integrated luminosity in the same year.

Fig. 6 summarizes daily integrated luminosity (top) and integrated luminosity (bottom) during the SIDDHARTA data taking, which ended at the beginning of November 09. The integrated

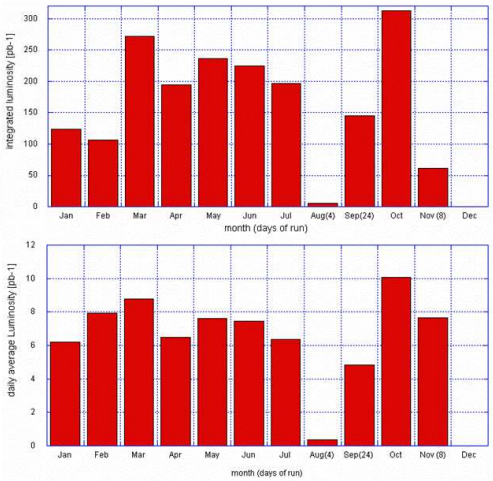

Figure 5: SIDDHARTA Integrated Luminosity (see text).

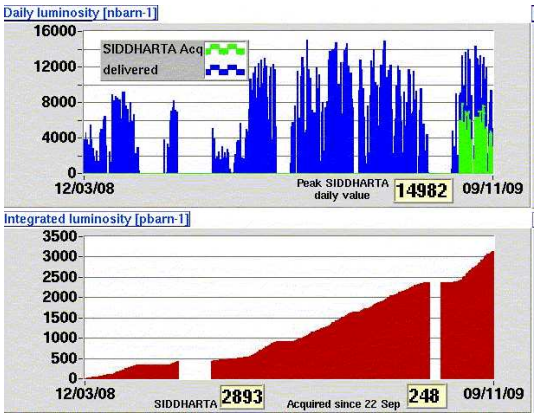

Figure 6: SIDDHARTA Integrated Luminosity (see text).

luminosity profited from implementing a new software procedure to switch the injection system from electrons to positrons and the other way round. The switch time has been reduced by a factor three and now it is less than one minute.

A continuos injection regime provides L $\approx$ 1 pb^{-1} hourly integrated luminosity, which is not compatible with the SIDDHARTA experiment data taking since the acquisition is vetoed during injection due the higher background level. However this result opens significant perspectives for the KLOE experiment, which is much less sensitive to background. The best integrated luminosity obtained in a moderate injection regime compatible with the SIDDHARTA operation with a $\approx$ 50% duty cycle is L $\approx$ .79 pb^{-1} hourly averaged over two hours.

DAΦNE luminosity as a function of the colliding bunches compared to past runs is reported in Fig. 7. Blue and red dots refer to the two KLOE runs, with the initial triplet low-β IR quadrupoles and with the new IR doublet, respectively. Yellow dots refer to the FINUDA run; in green is the luminosity with the CW scheme. The gain provided by the new IR gets higher with the products of the currents and the difference with respect to collisions with the crab sextupoles off can reach 50%.

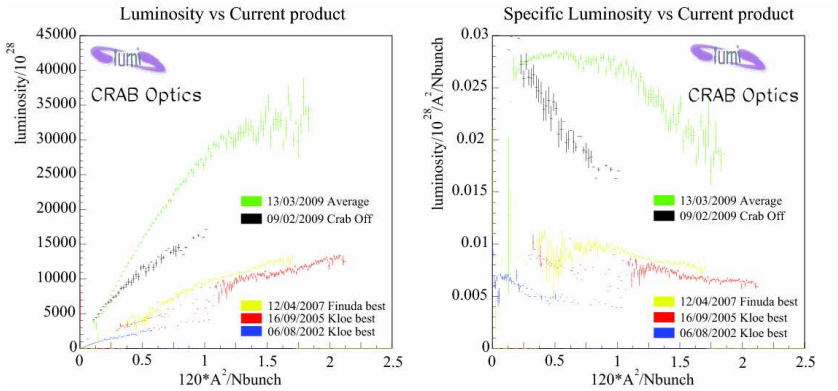

Figure 7: (color online). Comparison of the upgraded DAΦNE perfomance (green) with respect to the results during previuos KLOE (blue, red) and FINUDA runs (yellow).

Table 2: Present DAΦNE luminosity performances with the CW scheme and low-β parameters compared to the KLOE and FINUDA runs. SIDDHARTA data taking does not profit of the fast injection rate system, that would increase $L_{\int logged}$.

	SIDDHARTA March 08÷Nov 09	KLOE May 04÷Nov 05	FINUDA Nov 06÷Jun 07
L_{peak} [cm^{-2}s^{-1}]	4.5	1.5	1.6
$L^{MAX}_{\int day}$ [pb^{-1}]	15.24	9.8	9.4
$L^{MAX}_{\int hour}$ [pb^{-1}]	1.033	0.44	0.5
$I^{-\ MAX}_{coll}$ [A]	1.4	1.4	1.5
$I^{+\ MAX}_{coll}$ [A]	1	1.2	1.1
$n_{bunches}$	105	111	106
$L_{\int logged}$ [fb^{-1}]	2.9	2.0	0.966
β^*_x [m]	0.25	1.5	2.0
β^*_y [m]	0.009	0.018	0.019
ϵ_x [10^{-6} m $\cdot$ rad]	0.25	0.34	0.34
ξ_y	0.0443	0.025	0.029

During 2009 the peak luminosity has been progressively improved by tuning the collider and increasing the beam currents; the maximum value achieved is $\approx 4.5 \times 10^{32}$ cm^{-2}s^{-1} measured in several runs with good luminosity to background ratio. The present peak luminosity is close to the nominal one predicted by numerical simulations. The highest single bunch luminosity achieved is $\approx 5 \times 10^{30}$ cm^{-2}s^{-1} measured with 20 bunches in collisions instead of the usual 105. The single bunch specific luminosity, defined as the single bunch luminosity divided by the product of the single bunch currents, at low currents exceed by 4 times the best value measured during the past DAΦNE runs (present values are red and blue dots in Fig. 8). It gradually decreases with colliding beam currents, as can be seen in Fig. 8. This reduction can be only partially explained by the growing beam size blow up due to the beam-beam interaction. Another factor comes from the fact that in the large Piwinski angle regime the luminosity decreases with the bunch length, which in turn is affected by the ring coupling impedance.

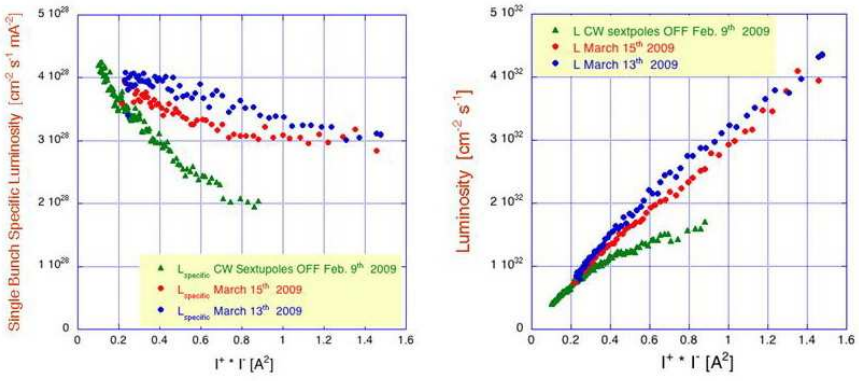

Figure 8: (color online). Single bunch specific luminosity (left) and luminosity (right) versus the product of the colliding currents for two of the best run and for the crab waist sextupoles off.

The impact of the Crab-Waist sextupoles can be recognized comparing runs taken with CW sextupoles on and off (Fig. 8). At low current the luminosity is the same in the two cases and higher than the one measured with the original collision scheme. As the product of the stored currents exceed 0.3 A, the luminosity with CW sextupoles off becomes lower and a corresponding transverse beam size blow up and beam lifetime reduction are observed as a consequence of the uncompensated beam-beam resonances.

The convolved vertical beam size at the IP in collision has been measured by means of a beam-beam scan technique. The measured Σ_y of 5.6 μm is compatible with the value obtained by using the coupling value (k=0.7%) as measured at the Synchrotron Light Monitor (SLM), being the single vertical beam size at the IP1 of the order of 4 μm.

Fig. 9 reports another proof of the crab sextupoles effectiveness, where the positrons transverse beam profile measured at the synchrotron light monitor with crab sextupoles OFF (left plot) and with crab sextupoles ON (right plot) is shown. The measurement refers to collision in a strong-weak regime (1 A electrons beam current against 0.1 A of positrons beam current): it is evident that the transverse beam size is smaller and its shape remains Gaussian during collision with the sextupoles ON.

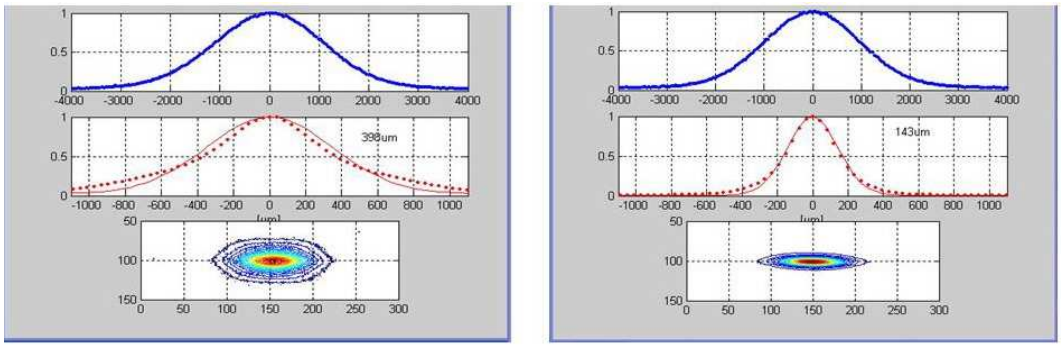

Figure 9: Transverse positron beam profile as measured at SLM with crab sextupoles off (left) and crab sextupoles on (right) for beams in collisions (103 bunches).

The crab waist sextupoles proved to be of great importance for the collider luminosity increase, since much lower luminosity is achieved with crab sextupoles off, with a larger blow up and a sharp lifetime reduction is observed for single bunch currents greater than 8-10 mA. This is in agreement with beam-beam simulations taking into account the DAΦNE nonlinear lattice. The results achieved at DAΦNE have pushed several accelerator teams to study and consider the implementation of this scheme on their machines. Besides, the physics and the accelerator communities are discussing a new project of a Super B-factory with luminosity as high as 10^{36} cm^{-2}s^{-1}, i.e. by about two orders of magnitude higher with respect to that achieved at the existing B-factories at SLAC and KEK.

6 Future Activities in view of the KLOE run

The new collision scheme based on large Piwinski angle and Crab Waist implemented on DAΦNE worked as predicted by the preliminary studies and numerical simulations. The present luminosity achievements opened new perspectives for the DAΦNE collider and a new run for the KLOE

experiment has been planned for the year 2010. During 2009 the new interaction region design for KLOE has been completed and several components of the new hardware have been acquired. Main improvements with respect to the present optics and past KLOE run are:

- increased beam stay clear at the IR;
- better shielding;
- additional skew quadrupoles added across QF1;
- independent pair of anti-solenoids for each beam;

Due to the larger crossing angle, the vertical displacement of the beam in the IR is about an order of magnitude larger than the last KLOE run. A system of permanent magnet dipoles compatible with different fields of the KLOE detector has been designed and built to be installed after each QF1 to keep under control the vertical beam trajectory.

Hardware activities to allow the new KLOE run have been started immediately after the end of the SIDDHARTA run.

The LINAC gun cathode, almost exausted, will be replaced with a new one and a further accelerating section will be added at the end to improve stability during operation for positrons.

Stripline electrodes will be installed in all wigglers and dipole vacuum chamber for electron cloud clearing. The horizontal feedback power will be doubled and the horizontal feedback kicker will be modified to improve feedback effectiveness.

Wigglers magnet will be modified according to a novel technique that will improve the good field region. It will increase the manimum field for a given current and decrease the wall plug power. In the modified wiggler the beam trajectory passes always near the pole center, in this way the higher order terms in the magnetic field are significantly reduced.

Remaining old type bellow are being replaced with a modified one which have lower impedance and better mechanical performance. All remaining ions clearing electrodes in the electron ring will be removed. Fast kickers will be installed to dump the beams on a single turn basis in a clean way upon operator request or hardware failure, to reduce detector trips and radiation interlocks. A new low level RF feedback is under development to improve longitudinal stability reducing at the same time the wall plug power. The shutdown for the KLOE roll-in is foreseen to end on spring 2010, an overall improvement of the peak luminosity of the order of 20% with respect to the Siddharta one and an integrated luminosity of ≈ 0.5 fb^{-1} per month is expected after the initial commissioning.

7 Publications

1. M. Zobov et al., *Crab Waist Collision Scheme: Numerical Simulations versus Experimental Results*, Proc. of PAC09, Vancouver, (2009).

2. C. Milardi for the DAΦNE Collaboration Team: *Experience with DAΦNE Upgrade Including Crab Waist*, Proc. of PAC09, Vancouver, (2009).

3. T. Demma et al., *A Simulation Study of the Electron Cloud Instability at DAΦNE*, Proc. of PAC09, Vancouver, (2009).

4. A. Drago, *Fast Horizontal e+ Instability Measurements in DAΦNE*", Proc. of PAC09, Vancouver, (2009).

5. A. Drago, *DAΦNE Horizontal Feedback Upgrade*, Proc. of PAC09, Vancouver, 2009.

6. F. Marcellini et al., *Tests and Operational Experience with the DAΦNE Stripline Injection Kicker*, Proc. of PAC09, Vancouver (2009).

7. A. Stella et al., *Beam Tests with Libera in Single Pass Mode*, Proc. of DIPAC09, Basel(CH), (2009).

8. P. Valente et al., *Detectors for Absolute Luminosity Measurement at DAΦNE*, Proc. of DIPAC09, Basel (CH), (2009).

9. C. Milardi et al., *Results from the DAΦNE high luminosity test*, Nuovo Cimento C **32**, 379 (2009).

10. T. Demma et al., *Update of the electron cloud simulations for DAΦNE*, ICFA Beam Dyn. Newsletter **50**, 33 (2009).

11. M. Zobov et al., *Update Beam dynamics in crab waist collisions at DAΦNE*, ICFA Beam Dyn. Newsletter **48**, 34 (2009).

12. T. Demma et al., *Update Electron cloud simulations for DAΦNE*, ICFA Beam Dyn.Newsletter **48**, 64 (2009).

13. C. Milardi et al., *Crab waist collision at DAΦNE*, ICFA Beam Dyn. Newsletter **48**, 23 (2009).

14. M. Boscolo, *Touschek backgrounds experience at DAΦNE*, ICFA Beam Dyn. Newslett. **48**, 59 (2009).

15. C. Milardi et al., Int. J. Mod. Phys. A **24**, 360 (2009).

16. A. Drago, *Horizontal instability measurements and cure in DAΦNE*, ICFA Beam Dyn. Newsletter **48**, 50 (2009).

17. F. Marcellini et al., *The new DAΦNE kickers*, ICFA Beam Dyn. Newsletter **48**,45, (2009).